

# OMP: One-step Meanflow Policy with Directional Alignment

Han Fang<sup>1</sup> Yize Huang<sup>2</sup> Yuheng Zhao<sup>1</sup> Paul Weng<sup>3</sup> Xiao Li<sup>2</sup> Yutong Ban<sup>1</sup>

## Abstract

Robot manipulation, a key capability of embodied AI, has turned to data-driven generative policy frameworks, but mainstream approaches like Diffusion Models suffer from high inference latency and Flow-based Methods from increased architectural complexity. While simply applying meanFlow on robotic tasks achieves single-step inference and outperforms FlowPolicy, it lacks few-shot generalization due to fixed temperature hyperparameters in its Dispersive Loss and misaligned predicted-true mean velocities. To solve these issues, this study proposes an improved MeanFlow-based Policies: we introduce a lightweight Cosine Loss to align velocity directions and use the Differential Derivation Equation (DDE) to optimize the Jacobian-Vector Product (JVP) operator. Experiments on Adroit and Meta-World tasks show the proposed method outperforms MP1 and FlowPolicy in average success rate—especially in challenging Meta-World tasks—effectively enhancing few-shot generalization and trajectory accuracy of robot manipulation policies while maintaining real-time performance, offering a more robust solution for high-precision robotic manipulation.

## 1. Introduction

Robot manipulation, a cornerstone of embodied AI, empowers machines to interact with the physical world, executing tasks ranging from daily household chores (e.g., grasping utensils) to precise industrial operations (e.g., assembly) (Rajeswaran et al., 2018; Yu et al., 2019). With the rapid advancement of generative modeling, robot learning has transitioned from traditional supervised regression to data-driven generative policy frameworks. These frameworks excel at capturing complex, multimodal action distributions

<sup>\*</sup>Equal contribution <sup>1</sup>Global College, Shanghai Jiao Tong University, Shanghai, China <sup>2</sup>School of Mechanical Engineering, Shanghai Jiao Tong University, Shanghai, China <sup>3</sup>Duke Kunshan University, Jiangsu, China. Correspondence to: Yutong Ban <yban@sjtu.edu.cn>.

Preprint. Under review.

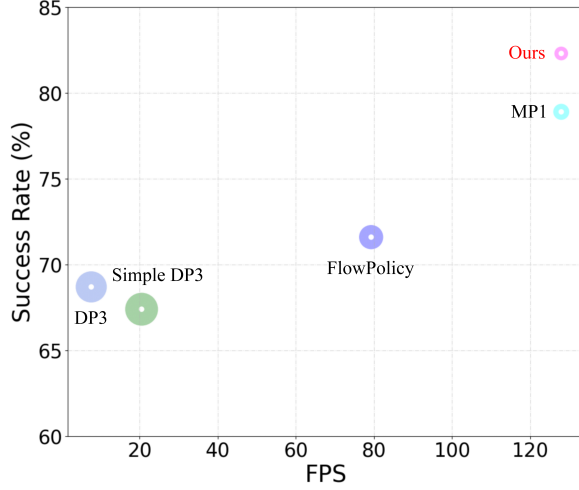


**Figure 1. Inference Speed vs. Success Rate Trade-off.** We compare our proposed OMP against state-of-the-art Diffusion-based methods (DP3, Simple DP3) and Flow-based methods (FlowPolicy, MP1). The x-axis represents control frequency in Frames Per Second (FPS), while the y-axis shows the average success rate (%) across Adroit and Meta-World tasks. The radius of each circle denotes the standard deviation across three random seeds.

and adapting to dynamic environments (Chi et al., 2023; Zhang et al., 2025). Currently, two paradigms dominate this landscape: Diffusion Models and Flow-based Methods, though both face significant trade-offs regarding real-time deployment and architectural complexity.

Diffusion Models, represented by Diffusion Policy (DP) (Chi et al., 2023) and its 3D extension DP3 (Ze et al., 2024), model robot actions as probabilistic denoising processes. By iteratively refining Gaussian noise into valid trajectories—particularly when conditioned on 3D point clouds—they achieve high success rates (Ze et al., 2024). However, their reliance on multi-step inference (e.g., Number of Function Evaluations (NFE) = 10 for DP3) results in prohibitive inference latency (e.g.,  $\sim 132$  ms on Adroit), rendering them unsuitable for real-time control tasks where millisecond-level responsiveness is critical.

Conversely, Flow-based Methods, such as AdaFlow (Hu et al., 2025b) and FlowPolicy (Zhang et al., 2025), address this inefficiency by learning vector fields to transform noise

into actions via Ordinary Differential Equations (ODEs), enabling single-step inference. While FlowPolicy reduces average inference time to  $\sim 20$  ms on Adroit and maintains competitive performance (Zhang et al., 2025), most flow-based approaches require explicit consistency constraints or segmented training. These requirements introduce architectural complexity and potential over-constraints that hinder generalization to novel scenes (Sheng et al., 2025).

A recent breakthrough, MeanFlow (Geng et al., 2025b), offers a new avenue by modeling interval-averaged velocity via its proposed MeanFlow Identity, eliminating the need for ODE solvers. MP1 (Sheng et al., 2025), the first adaptation of MeanFlow to robotics, achieves single-step inference (NFE=1) with an average latency of 6.8 ms (19 $\times$  faster than DP3) and outperforms FlowPolicy by 7.3% in average success rate. However, MP1 suffers from two critical limitations. First, its derivation relies on the model to predict instantaneous velocity, yet the model is trained on interval-averaged velocities. This discrepancy leads to inaccurate instantaneous predictions. Meanwhile, the derived identity requires the Jacobian-Vector Product (JVP) operator, which incurs high GPU memory consumption.

To address these challenges, we propose OMP, which introduces the following contributions:

- We design a lightweight direction alignment to align the direction of predicted interval-averaged velocities with true mean velocities. This resolves trajectory inaccuracies without increasing network depth.
- We apply a Differential Derivation Equation (DDE) to approximate Jacobian-Vector Product (JVP) computations, significantly reducing GPU memory consumption for complex tasks.
- We conduct extensive experiments on Adroit and Meta-World. Results demonstrate that OMP outperforms SOTA methods like MP1, specifically enhancing performance on challenging tasks.

## 2. Related Work

### 2.1. Visual Input Modalities in Robot Learning

Robot policy learning relies on visual modalities to perceive environmental states. Early frameworks utilized 2D RGB or depth images due to low computational costs, with methods like BC-Z (Jang et al., 2022) aligning visual-language features for zero-shot generalization. ALOHA (Zhao et al., 2023) employed ACT networks to model 2D vision-action relationships, and Diffusion Policy (DP) (Chi et al., 2023) utilized denoising processes for multimodal action modeling. However, 2D inputs often lack the explicit depth information required for high-precision tasks like stacking.

To address spatial ambiguity, 3D modalities like point clouds have become prevalent. Early 3D methods like PerACT (Shridhar et al., 2022) and ACT3D (Gervet et al., 2023) used voxel data but suffered from high memory costs. In contrast, methods such as RVT (Goyal et al., 2023), RVT-2 (Goyal et al., 2024) and DP3 (Ze et al., 2024) leverage Farthest Point Sampling (FPS) to preserve spatial structure while maintaining efficiency, significantly outperforming 2D baselines. Recent work has further enhanced this paradigm by integrating language-aligned 3D keypoints. For instance, CLAP (Hu et al., 2025a) employs a coarse-to-fine hierarchical policy that utilizes VLM-guided 3D keypoint prediction to improve generalization to novel instructions and environmental variations. FlowPolicy (Zhang et al., 2025) further integrated 3D point clouds with consistency flow matching, achieving single-step inference (NFE=1) and 70.0% average success rate on 37 tasks. MP1 (Sheng et al., 2025) combined 3D point clouds with MeanFlow, demonstrating that 3D inputs enhance the model’s ability to capture subtle scene variations (e.g., door handle position in Adroit Door task). Despite these advances, existing 3D-based flow methods (e.g., FlowPolicy) still require consistency constraints to ensure trajectory validity, while MeanFlow-based MP1 lacks adaptive mechanisms for few-shot scenarios—gaps addressed by our OMP.

### 2.2. Generative Models for Robot Policy Learning

Generative modeling has transformed robot learning by treating action generation as a probabilistic process. This landscape is currently defined by the trade-off between the high-fidelity generation of Diffusion Models and the inference speed of Flow-based Methods.

**Diffusion Models.** These models simulate data generation by denoising random Gaussian noise. DP (Chi et al., 2023) and its 3D extension, DP3 (Ze et al., 2024), have achieved high success rates by iteratively refining trajectories. Subsequent variants like HDP (Ma et al., 2024) and RDT (Liu et al., 2025) enhanced spatial modeling and dual-arm manipulation, respectively. Recent advancements continue to refine this paradigm. MTDP (Wang et al., 2025) improves action quality by modulating Transformer-based diffusion policies, while World4RL (Jiang et al., 2025b) utilizes diffusion world models for policy refinement to boost few-shot generalization. Parallel to these generative approaches, TR-DRL (Jiang et al., 2025a) enhances reinforcement learning efficiency for robotic manipulations by exploiting time reversal symmetry in temporally symmetric tasks. However, despite these improvements in quality and generalization, diffusion models inherently suffer from high inference latency due to multi-step denoising (e.g., NFE=10 for DP3), creating a bottleneck for real-time control.

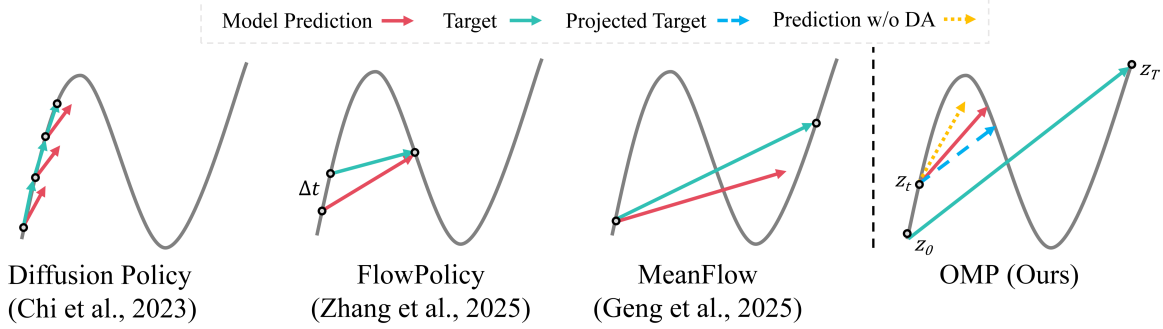


**Figure 2. Schematic Comparison of Generative Policy Trajectories.** This diagram contrasts the denoising processes of mainstream paradigms. DP3 requires multi-step denoising (10-NFE). FlowPolicy uses segmented straight-line flows but requires consistency constraints. Mean Policy predicts interval-averaged velocity but may suffer from misalignment between the predicted and target velocities due to training discrepancies. Our proposed OMP introduces Directional Alignment via a Cosine Loss, forcing the predicted velocity vector to align explicitly with the true mean velocity direction, ensuring trajectory accuracy in a single step.

**Flow-based Models.** To resolve latency issues, Flow-based models learn invertible mappings via vector fields. Traditional flow methods like AdaFlow (Hu et al., 2025b) used variance-adaptive flows for imitation learning but required variable NFEs. Consistency Flow Matching (Yang et al., 2024) addressed this by defining straight-line flows from any time step to the target action space, leading to FlowPolicy (Zhang et al., 2025) and ManiFlow (Yan et al., 2025), which employ consistency flow matching to enable single-step inference, though they often require explicit consistency constraints.

A clearer path to efficiency is offered by MeanFlow-based paradigms. MP1 (Sheng et al., 2025) adapted MeanFlow (Geng et al., 2025b) to robotics, using interval-averaged velocity fields to eliminate ODE solvers and achieve 6.8ms latency. Closely related to our work, DM1 (Zou et al., 2025) also focuses on one-step manipulation using MeanFlow with dispersive regularization. However, both MP1 and DM1 rely on training objectives that may allow the predicted velocity direction to drift from the true mean velocity (the straight line from noise to expert action). Unlike DM1, OMP introduces a specific Directional Alignment (Cosine Loss) to force vector alignment and utilizes a Differential Derivation Equation (DDE) to approximate JVP, simultaneously improving trajectory accuracy and reducing memory consumption compared to these predecessors.

### 3. Background

**Diffusion Model.** Diffusion models (DM) are generative models that model  $p_{\text{data}}(\mathbf{x})$  via stochastic forward/reverse diffusion. The forward process adds noise to  $\mathbf{x}_1 \sim p_{\text{data}}(\mathbf{x})$  over  $T$  steps to reach  $\mathbf{x}_T \sim \mathcal{N}(\mathbf{0}, \mathbf{I})$ :

$$\mathbf{x}_t = \sqrt{\alpha_t} \mathbf{x}_{t-1} + \sqrt{1 - \alpha_t} \boldsymbol{\epsilon}_t, \quad (1)$$

where  $\alpha_t$  is a noise schedule and the noise  $\boldsymbol{\epsilon}_t \sim \mathcal{N}(\mathbf{0}, \mathbf{I})$ . The reverse process learns  $\boldsymbol{\epsilon}_\theta(\mathbf{x}_t, t)$  to invert diffusion, minimizing  $\|\boldsymbol{\epsilon} - \boldsymbol{\epsilon}_\theta(\mathbf{x}_t, t)\|^2$ . DM models multimodal distributions but suffer from slow sampling.

Flow matching (FM) addresses DM inefficiency via a deterministic flow  $\mathbf{f}(\mathbf{x}, t)$  transforming  $p_0(\mathbf{x})$  to  $p_{\text{data}}(\mathbf{x}) = p_1(\mathbf{x})$ . The flow satisfies the continuity equation:

$$\frac{\partial p_t(\mathbf{x})}{\partial t} = -\nabla \cdot (p_t(\mathbf{x}) \mathbf{f}(\mathbf{x}, t)), \quad (2)$$

where  $p_t(\mathbf{x})$  is the distribution at time  $t$ . FM enables fast sampling, which usually contains tens of ODE steps.

These methods optimize DMs for sampling in  $T = 1$  or  $T \ll 100$  steps. Recently, one-step models have drawn increase attention for its faster sampling speed. Those one-step models use a decoder  $\boldsymbol{\theta}$  to map  $\mathbf{x}_T$  directly to  $\mathbf{x}_1$ . They balance speed and quality, making them suitable for robotic tasks that require low latency.

**Diffusion-based Policy.** Diffusion-based policies adapt diffusion models to policy learning, modeling state-to-action distribution  $\pi(\mathbf{a} \mid \mathbf{s})$  as the target of a state-conditioned diffusion process. Actions are sampled via ODE solving or direct decoding. These policies learn from demonstrations and can handle high-dimensional actions.

### 4. Method

Our work builds upon the MeanFlow framework, a robot learning paradigm that achieves single-step trajectory generation using 3D point-cloud inputs. While the original MeanFlow implementation in robotics, MP1, successfully eliminates Ordinary Differential Equation (ODE) solver errors by learning interval-averaged velocities, we identify critical theoretical limitations in how these models optimize

high-precision tasks. Specifically, the reliance on standard Mean Squared Error (MSE) loss leads to gradient starvation in low-velocity regimes. To address this, we introduce the One-step Meanflow Policy (OMP), which incorporates a geometric analysis of high-dimensional error landscapes to motivate a novel Directional Alignment objective and utilizes a Differential Derivation Equation to optimize computational efficiency MeanFlow Framework.

#### 4.1. Meanflow Framework

We first recapitulate the MeanFlow framework to establish the necessary notation. The core innovation of MeanFlow lies in directly learning interval-averaged velocities  $u(z_t, r, t)$  rather than the instantaneous velocities used in standard Flow Matching. This formulation circumvents the need for multi-step numerical integration, enabling single-step inference ( $NFE = 1$ ) essential for real-time robotic control. In this setting, the inference process aims to recover a clean sample  $z_0$  from an initial noise batch  $z_T \sim \mathcal{N}(0, I)$  in a single step. The true mean velocity  $v_0$  is defined as the direct vector connecting the noise to the target:

$$v_0 \triangleq z_T - z_0. \quad (3)$$

During training, the model  $u_\theta(z_t, r, t|c)$ , conditioned on context  $c$ , is optimized using the MeanFlow Identity. This identity relates the total derivative of the velocity to the discrepancy between the instantaneous and average velocities:

$$u(z_t, r, t|c) = v(z_t, t|c) - (t - r) \frac{d}{dt} u(z_t, r, t|c). \quad (4)$$

The right-hand side of this identity serves as the target velocity  $u_{tgt}$  for the parameterized network. The standard training objective minimizes the Mean Squared Error (MSE) between the prediction and this target, often augmented by a Dispersive Loss  $\mathcal{L}_{Disp}$  (Geng et al., 2025a) to encourage feature discrimination within the latent space.

#### 4.2. The Geometry of High-Dimensional Error Landscapes

To understand the necessity of our proposed Directional Alignment, we must examine the gradient dynamics of the MSE loss function in high-dimensional vector regression. Let  $u \in \mathbb{R}^d$  be the predicted velocity and  $u^* \in \mathbb{R}^d$  be the target velocity. The MSE loss is defined as:

$$\mathcal{L}_{MSE} = \|u - u^*\|_2^2. \quad (5)$$

The gradient with respect to the prediction is  $\nabla_u \mathcal{L}_{MSE} = u - u^*$ . We can decompose this error vector into a radial component (magnitude error) and a tangential component (directional error). Let  $u = \rho \hat{n}$  and  $u^* = \rho^* \hat{n}^*$ , where  $\rho, \rho^*$  are scalars and  $\hat{n}, \hat{n}^*$  are unit vectors. The MSE can be rewritten using the Law of Cosines:

$$\mathcal{L}_{MSE} = \rho^2 + (\rho^*)^2 - 2\rho\rho^* \cos \alpha, \quad (6)$$

where  $\alpha$  is the angle between  $u$  and  $u^*$ . The derivative of the loss with respect to the angle  $\alpha$  is:

$$\frac{\partial \mathcal{L}_{MSE}}{\partial \alpha} = 2\rho\rho^* \sin \alpha. \quad (7)$$

This equation reveals a critical pathology: the gradient signal for correcting the direction ( $\alpha$ ) is proportional to the product of the magnitudes  $\rho$  and  $\rho^*$ . This proportionality has severe implications for robotic manipulation. In tasks requiring high precision, such as "Peg Insert" or "Thread in Hole", the required velocity  $u^*$  approaches zero ( $\rho^* \rightarrow 0$ ). As the target magnitude shrinks, the gradient  $\frac{\partial \mathcal{L}}{\partial \alpha}$  vanishes. Consequently, the network effectively stops learning the direction of movement for fine manipulation tasks, focusing only on minimizing the magnitude error. This explains why standard flow models often fail to converge on high-precision tasks. Furthermore, if the training dataset contains a mix of large motions and small motions, the gradients from the large motions will dominate the updates. The optimization trajectory becomes biased towards minimizing errors in high-velocity regions, leaving the directional accuracy of low-velocity regions under-optimized.

#### 4.3. Directional Alignment

To mitigate the gradient starvation issue identified in the error landscape analysis, we propose a Directional Alignment mechanism. The MeanFlow framework allows a single network to calculate both instantaneous and average velocities. However, because the model is trained on arbitrary time intervals, it inherently struggles to predict accurate instantaneous velocities. As derived in Equation (4), inaccuracies in the instantaneous prediction propagate to the target velocity  $u_{tgt}$ , leading to accumulated errors. We address this by enforcing an explicit alignment between the predicted average velocity  $u(z_t, r, t|c)$  and the true mean velocity  $v_0$ . Unlike the MSE loss, which couples magnitude and direction, we introduce a Cosine Loss that isolates the directional component. The cosine of the angle  $\alpha$  between the prediction and the ground truth is calculated as:

$$\cos \alpha = \frac{v_0 \cdot u(z_t, r, t|c)}{\|v_0\| \cdot \|u(z_t, r, t|c)\|}. \quad (8)$$

We formulate the Cosine Loss  $\mathcal{L}_{cos}$  to maximize this alignment:

$$\mathcal{L}_{cos} = -\log \left( \frac{\cos \alpha + 1}{2} \right). \quad (9)$$

By incorporating this term, the final training objective becomes a weighted sum of the reconstruction, dispersive, and cosine losses:

$$\mathcal{L} = \mathcal{L}_{mse} + \lambda_{Disp} \cdot \mathcal{L}_{Disp} + \lambda_{cos} \cdot \mathcal{L}_{cos}. \quad (10)$$

This objective ensures that the predicted velocity vector aligns with the straight-line path from noise to expert action,

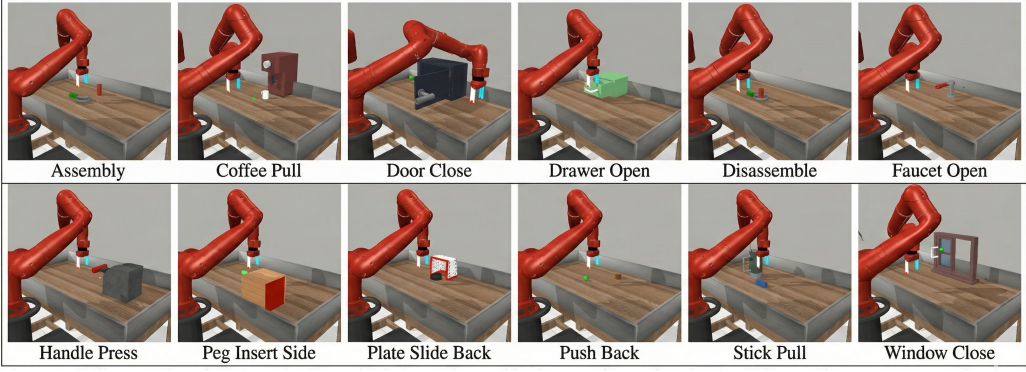


**Figure 3. Simulation Benchmark Environments.** Visualizations of the diverse manipulation tasks used for evaluation. We test on the high-precision Adroit benchmark and the multi-task Meta-World benchmark, covering a total of 37 distinct tasks ranging from simple household interactions to complex tool use.

even when the velocity magnitude is negligible, effectively countering the gradient starvation phenomenon.

#### 4.4. Optimization of JVP Operator

While Directional Alignment improves trajectory accuracy, the computational cost of the MeanFlow Identity remains a challenge. The calculation of the target velocity involves partial derivatives that are typically computed using the Jacobian-Vector Product (JVP) operator. This operator incurs high GPU memory consumption, creating a bottleneck when training on complex tasks with high-dimensional inputs. To resolve this memory constraint, we implement a Differential Derivation Equation (DDE) to approximate the JVP computations. We approximate the time derivative of the network output using a finite difference method:

$$\frac{du_\theta(z_t, t, r|c)}{dt} \approx \frac{u_\theta(z_t, t + \epsilon, r|c) - u_\theta(z_t, t, \epsilon, r|c)}{2\epsilon}, \quad (11)$$

where  $\epsilon$  is a small perturbation constant. This approximation significantly reduces memory usage by obviating the need to store intermediate Jacobian variables during the backward pass. Although DDE introduces a minor approximation error, our empirical results suggest it maintains satisfactory prediction performance while making the training of complex, high-precision policies computationally feasible.

## 5. Experimental Results

**Dataset and Tasks.** As shown in Figure 3, we evaluate our proposed method on multiple tasks, including 3 from the Adroit benchmark and 34 tasks from the Meta-World benchmark. The tasks from the Meta-World Benchmark can be classified into twenty-one Easy tasks, four Medium tasks, four Hard tasks and five Very Hard tasks.

**Baselines.** We compare our proposed OMP with multiple SOTA Baselines, including DP, AdaFlow, and CP with 2D inputs, as well as DP3, Simple DP3, FlowPolicy, and MP1 with 3D inputs. DP, DP3, and Simple DP3 all employ multi-step inference (NFE=10), whereas CP and FlowPolicy use single-step inference (NFE=1), and AdaFlow operates with a variable NFE.

**Experimental Setup.** To train on Adroit and Meta-World tasks, we generate 10 expert demonstrations for each simulation task. When dealing with point-cloud data, we use the Farthest Point Sampling (FPS) strategy to reduce the number of points to either 512 or 1024, while for image data, we downsample the resolution to  $84 \times 84$  pixels. All evaluated baselines and OMP are assessed through three experiments, each corresponding to a different random seed (0, 1, and 2), and in each experiment, the evaluated method is required to train for 3000 epochs per task on Adroit and 1000 epochs per task on Meta-World. Performance is evaluated every 200 epochs, with final performance calculated as the average of the five highest success rates, and the overall success rate and standard deviation for each task are computed across all three experiments. All training and testing procedures are performed on an NVIDIA RTX 4090 GPU with a batch size of 128, and for optimization, we use the AdamW optimizer with a learning rate of 0.0001 (consistently applied to both Adroit and Meta-World), along with an observation window of 2 steps, a history length of 4 states, and a prediction horizon of 4 steps.

**Quantitative Evaluations.** Table 1 demonstrates that our proposed OMP achieves superior performance compared to SOTA baselines. OMP achieves an average performance of  $82.3\% \pm 1.7\%$ , outperforms the latest SOTA method mp1, which achieves an average performance of  $78.9\% \pm 2.1\%$ . OMP yields a 3.4% improvement over mp1 and a 10.7% improvement over Flowpolicy. The improvement of the aver-

Methods	NFE	Adroit			Meta-World				Average
		Hammer	Door	Pen	Easy (21)	Medium (4)	Hard (4)	Very Hard (5)	
DP(RSS'23)	10	16±10	34±11	13±2	50.7±6.1	11.0±2.5	5.25±2.5	22.0±5.0	35.2±5.3
Adaflow(NeurIPS'24)	-	45±11	27±6	18±6	49.4±6.8	12.0±5.0	5.75±4.0	24.0±4.8	35.6±6.1
CP(arxiv'24)	1	45±4	31±10	13±6	69.3±4.2	21.2±6.0	17.5±3.9	30.0±4.9	50.1±4.7
DP3(RSS'24)	10	100±0	56±5	46±10	87.3±2.2	44.5±8.7	32.7±7.7	39.4±9.0	68.7±4.7
Simple DP3(RSS'24)	10	98±2	40±17	36±4	86.8±2.3	42.0±6.5	38.7±7.5	35.0±11.6	67.4±5.0
FlowPolicy(AAAI'25)	1	98±1	61±2	54±4	84.8±2.2	58.2±7.9	40.2±4.5	52.2±5.0	71.6±3.5
MPI(arxiv'25)	1	100±0	69±2	58±5	88.2±1.1	68.0±3.1	58.1±5.0	67.2±2.7	78.9±2.1
OMP(Ours)	1	100±0	68±3	60±4	89.7±0.7	77.4±2.2	62.5±3.1	77.8±3.0	82.3±1.7

Table 1. Main Results on Adroit and Meta-World Benchmarks. A comprehensive performance comparison across 37 tasks using 3 random seeds. NFE denotes the Number of Function Evaluations required for inference (lower is faster).

Methods	Adroit			Meta-World				Average
	Hammer	Door	Pen	Easy (21)	Medium (4)	Hard (4)	Very Hard (5)	
OMP	100±0	68±3	60±4	89.7±0.7	77.4±2.2	62.5±3.1	77.8±3.0	82.3±1.7
$-\mathcal{L}_{dis}$	100±0	69±2	58±4	89.1±1.0	76.8±3.1	57.8±4.2	75.0±3.7	81.2±2.0
$-\mathcal{JVP} + DDE$	100±0	68±2	64±3	89.0±1.3	76.4±2.7	61.0±3.0	70.6±4.9	80.8±2.2
$-\mathcal{L}_{dis} - \mathcal{L}_{cos}$	95±5	66±3	48±4	87.5±1.8	73.0±2.7	57.5±4.5	68.0±3.5	78.3±2.5

Table 2. Ablation Study of OMP Components. We analyze the impact of specific modules on the average success rate.  $-\mathcal{L}_{dis}$  denotes the removal of Dispersive Loss, and  $-\mathcal{L}_{cos}$  indicates the removal of our proposed Directional Alignment.

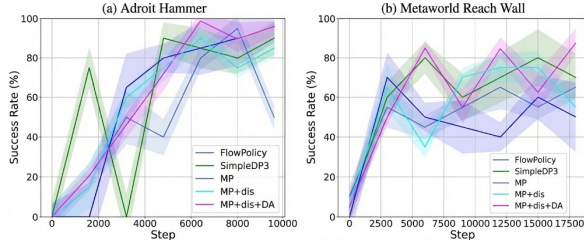


Figure 4. Training Stability and Convergence Analysis. Success rate curves during training for (a) Adroit Hammer and (b) Meta-World Reach Wall.

age performance over mp1 is not quite significant since mp1 achieves a near-optimal performance, i.e.,  $88.2\% \pm 1.1\%$  success rate, on Meta-World easy tasks, which contains the majority of simulation tasks, i.e., 21 tasks over totally 37 tasks. While we focus our attention on some poorly-performed tasks, like Meta-World Medium, Hard, and Very Hard tasks, our improvement over mp1 is significant. OMP yields a 9.4% improvement over Meta-World Medium tasks, a 4.4% improvement over Meta-World Hard tasks and a 10.6% improvement over Meta-World Very Hard tasks.

**Training Efficiency.** Figure 4 illustrates the training-phase success rate curves of baseline methods and our proposed OMP. While both the baseline methods and OMP show improvements in success rates over the course of training, the baseline methods exhibit a volatile trend during this process. By contrast, OMP maintains a high-level and relatively stable training trajectory. Additionally, OMP achieves faster convergence compared to all baseline methods, a benefit attributed to its additional guidance mechanism. We

have also overlaid a shadow area on each curve, which represents the standard deviation across different random seeds. This visualization further underscores the superior stability and robustness of OMP relative to the baseline methods.

**Ablation Study.** We also conduct ablation study experiments to verify the effects of each component. Our ablation study includes two extra experiments, where  $-\mathcal{L}_{dis}$  (resp.  $-\mathcal{L}_{cos}$ ) denotes removing the dispersive loss term during training (resp. removing the directional alignment) and  $-\mathcal{JVP} + DDE$  denotes using DDE to replace JVP operator. Based on Table 2, removing the Dispersive Loss term leads to a performance drop, but not too significant except on Hard tasks in Meta-world environment. Meanwhile, using DDE to replace JVP operator can cause some approximation errors, leading to a performance drop. However, considering the decreased GPU memory usage, the drop could be viewed as a tradeoff when implementing complex tasks. The performance drop led by removing the directional alignment is significant. Comparing the results of  $-\mathcal{L}_{dis}$  and  $-\mathcal{L}_{dis} - \mathcal{L}_{cos}$ , we can see a performance drop in all tasks on both Adroit and Meta-world environments, which verifies the significance of applying the directional alignment.

## 6. Conclusion

In this paper, we propose a novel and lightweight directional alignment to better train the Meanflow-based policies. Meanwhile, we propose to use the Differential Derivation Equation (DDE) to approximate the partial derivatives when facing complex tasks. Abundant experiments exhibit that our proposed OMP achieves a superior achievement compared to directly applying Meanflow to robotic areas.

## References

Chi, C., Feng, S., Du, Y., Xu, Z., Cousineau, E., Burchfiel, B. C., and Song, S. Diffusion policy: Visuomotor policy learning via action diffusion. volume 19, 2023. ISBN 978-0-9923747-9-2. URL <https://roboticsproceedings.org/rss19/p026.html>.

Geng, Z., Deng, M., Bai, X., Kolter, J. Z., and He, K. Diffuse and disperse: Image generation with representation regularization. *arXiv preprint arXiv:2506.09027*, 2025a. URL <https://arxiv.org/abs/2506.09027>.

Geng, Z., Deng, M., Bai, X., Kolter, J. Z., and He, K. Mean flows for one-step generative modeling, 2025b. URL <https://arxiv.org/abs/2505.13447>.

Gervet, T., Xian, Z., Gkanatsios, N., and Fragkiadaki, K. Act3d: 3d feature field transformers for multi-task robotic manipulation, 2023. URL <https://arxiv.org/abs/2306.17817>.

Goyal, A., Xu, J., Guo, Y., Blukis, V., Chao, Y.-W., and Fox, D. RVT: Robotic view transformer for 3d object manipulation, 2023. URL <https://arxiv.org/abs/2306.14896>.

Goyal, A., Blukis, V., Xu, J., Guo, Y., Chao, Y.-W., and Fox, D. RVT-2: Learning precise manipulation from few demonstrations, 2024. URL <https://arxiv.org/abs/2406.08545>.

Hu, J., Wang, L., Li, S., Jiang, Y., Li, X., Weng, P., and Ban, Y. Generalizable coarse-to-fine robot manipulation via language-aligned 3d keypoints. *arXiv preprint arXiv:2509.23575*, 2025a. doi: 10.48550/arXiv.2509.23575. URL <https://arxiv.org/abs/2509.23575>.

Hu, X., Liu, B., Liu, X., and Liu, Q. AdaFlow: imitation learning with variance-adaptive flow-based policies. In *Proceedings of the 38th International Conference on Neural Information Processing Systems*, volume 37 of *NIPS '24*, pp. 138836–138858. Curran Associates Inc., 2025b. ISBN 9798331314385.

Jang, E., Irpan, A., Khansari, M., Kappler, D., Ebert, F., Lynch, C., Levine, S., and Finn, C. BC-z: Zero-shot task generalization with robotic imitation learning, 2022. URL <https://arxiv.org/abs/2202.02005>.

Jiang, Y., Hu, J., Weng, P., and Ban, Y. Time reversal symmetry for efficient robotic manipulations in deep reinforcement learning. *arXiv preprint arXiv:2505.13925*, 2025a. doi: 10.48550/arXiv.2505.13925. URL <https://arxiv.org/abs/2505.13925>.

Jiang, Z. et al. World4rl: Diffusion world models for policy refinement with reinforcement learning for robotic manipulation. *arXiv preprint arXiv:2509.19080*, 2025b.

Liu, S., Wu, L., Li, B., Tan, H., Chen, H., Wang, Z., Xu, K., Su, H., and Zhu, J. RDT-1b: a diffusion foundation model for bimanual manipulation, 2025. URL <http://arxiv.org/abs/2410.07864>.

Ma, X., Patidar, S., Haughton, I., and James, S. Hierarchical diffusion policy for kinematics-aware multi-task robotic manipulation, 2024. URL <http://arxiv.org/abs/2403.03890>.

Rajeswaran, A., Kumar, V., Gupta, A., Vezzani, G., Schulman, J., Todorov, E., and Levine, S. Learning complex dexterous manipulation with deep reinforcement learning and demonstrations, 2018. URL <http://arxiv.org/abs/1709.10087>.

Sheng, J., Wang, Z., Li, P., and Liu, M. MP1: Mean-Flow tames policy learning in 1-step for robotic manipulation, 2025. URL <http://arxiv.org/abs/2507.10543>.

Shridhar, M., Manuelli, L., and Fox, D. Perceiver-actor: A multi-task transformer for robotic manipulation, 2022. URL <http://arxiv.org/abs/2209.05451>.

Wang, Q., Sun, Y., Lu, E., Zhang, Q., and Zeng, Y. Mtdp: A modulated transformer based diffusion policy model. *arXiv preprint arXiv:2502.09029*, 2025.

Yan, G., Zhu, J., Deng, Y., Yang, S., Qiu, R.-Z., Cheng, X., Memmel, M., Krishna, R., Goyal, A., Wang, X., and Fox, D. Maniflow: A general robot manipulation policy via consistency flow training. In *9th Annual Conference on Robot Learning (CoRL)*, 2025. URL <https://arxiv.org/abs/2509.01819>.

Yang, L., Zhang, Z., Zhang, Z., Liu, X., Xu, M., Zhang, W., Meng, C., Ermon, S., and Cui, B. Consistency flow matching: Defining straight flows with velocity consistency, 2024. URL <https://arxiv.org/abs/2407.02398>.

Yu, T., Quillen, D., He, Z., Julian, R. C., Hausman, K., Finn, C., and Levine, S. Meta-world: A benchmark and evaluation for multi-task and meta reinforcement learning. 2019. URL <https://www.semanticscholar.org/paper/Meta-World%20-%20A-Benchmark-and-Evaluation-for-and-Meta-Yu-Quillen-0bc855f84668b35cb65618d996d09f6e434d28c9>.

Ze, Y., Zhang, G., Zhang, K., Hu, C., Wang, M., and Xu, H. 3d diffusion policy: Generalizable visuomotor policy learning via simple 3d representations, 2024. URL <http://arxiv.org/abs/2403.03954>.

Zhang, Q., Liu, Z., Fan, H., Liu, G., Zeng, B., and Liu, S. FlowPolicy: enabling fast and robust 3d flow-based policy via consistency flow matching for robot manipulation. In *Proceedings of the Thirty-Ninth AAAI Conference on Artificial Intelligence and Thirty-Seventh Conference on Innovative Applications of Artificial Intelligence and Fifteenth Symposium on Educational Advances in Artificial Intelligence*, volume 39 of *AAAI'25/IAAI'25/EAAI'25*, pp. 14754–14762. AAAI Press, 2025. ISBN 978-1-57735-897-8. doi: 10.1609/aaai.v39i14.33617. URL <https://doi.org/10.1609/aaai.v39i14.33617>.

Zhao, T. Z., Kumar, V., Levine, S., and Finn, C. Learning fine-grained bimanual manipulation with low-cost hardware, 2023. URL <http://arxiv.org/abs/2304.13705>.

Zou, G. et al. Dm1: Meanflow with dispersive regularization for 1-step robotic manipulation. *arXiv preprint arXiv:2510.07865*, 2025.